

Feasibility of Electric Power Transmission by DC Superconducting Cables

P. Chowdhuri, Fellow, IEEE, C. Pallem, Student Member, IEEE, J.A. Demko and M.J. Gouge

Abstract--The electrical characteristics of dc superconducting cables of two power ratings were studied: 3 GW and 500 MW. Two designs were considered for each of the two power ratings. In the first design, the SUPPLY stream of the cryogen is surrounded by the high-voltage HTS cylinder. The RETURN stream of the cryogen is on the grounded side of the system. In the second design, both the SUPPLY and the RETURN streams of the cryogen are on the grounded side of the cable. Two electrical characteristics of these cables were studied: (1) fault current and (2) current harmonics. It was concluded that neither the fault currents nor the current harmonics pose any problems in the operation of the dc superconducting cables.

Index Terms – dc superconducting cable, high-temperature superconductivity, power transmission

I. INTRODUCTION

Increasing demand for electric power coupled with lack of corridors for power transmission and distribution has resulted in congestion in the power corridors with the attendant problem of instability in power delivery. Concurrently, the demand for higher power quality is increasing. Overhead power lines, being exposed to the elements of nature, are vulnerable to outages. However, overhead power lines have traditionally been built because of their cost advantages.

In spite of the cost effectiveness of the overhead power lines, the development of underground cables has been phenomenal during the entire twentieth century. The basic advantage of a superconducting cable is that it can transport the same amount of electric power as any other transport means but at lower voltage level. As the cost of power is a function of voltage, electric power transport by superconducting cable is a viable alternative. Also, the significantly higher power density in a superconducting cable than that in the other alternative power transport systems makes it an attractive means to transport cost-effective electric power over long distances.

This work was supported by the State of Tennessee, Department of Economic and Community Development under contract ED-03-01024-01 and the Center for Electric Power, Tennessee Technological University.

P. Chowdhuri (e-mail: pchowdhuri@tntech.edu) and C. Pallem (e-mail: cpallem21@tntech.edu) are with the Tennessee Technological University, Cookeville, TN 38505. J.A. Demko (e-mail: demkoja@ornl.gov) and M.J. Gouge (e-mail: gougemi@ornl.gov) are with the Oak Ridge National Laboratory, Oak Ridge, TN 37831

The refrigeration system of a superconducting cable is one of the principal items of the capital cost. The introduction of the high temperature superconductors (HTS) has increased the possibility of industrial application of superconducting cables significantly because (i) nitrogen as cryogen, in comparison to helium, is in abundant supply and therefore is inexpensive, and (ii) the efficiency of the higher temperature (77 K) nitrogen-cooled refrigeration system is considerably higher than the helium-cooled (10 K) refrigeration system.

Comparing ac and dc superconducting cables, the power-handling capability of an ac superconducting cable is limited by the stability limit of the power system; the dc superconducting cable has no such constraint. The charging current of an ac superconducting cable can be a significant fraction of the load current, particularly for long cables, thus reducing the power-handling capability of an ac cable considerably. A dc superconducting cable does not suffer from this constraint. An ac superconducting cable has hysteresis and eddy current losses in the superconductor and its stabilizer caused by the ac magnetic flux, in addition to the dielectric losses. These 'cold' temperature losses when translated to the room temperature, will demand higher refrigeration power to maintain the cable at the superconducting temperature. Moreover, the high fault-current level in the ac system may drive the superconductor to 'normal' which may cause damages to the superconductor. External fault current limiters may be required in the ac superconducting cable system to prevent the conductor from going normal. In fact, no ac circuit breaker exists today which can continuously carry the full-load current required for an ac superconducting cable, let alone the interruption of fault currents. A dc superconducting cable does not need a circuit breaker for point-to-point power transmission. The converters at either end of the dc cable will act as electronic circuit breakers, in addition to their primary function of power conversion. Because of the fast response time of the converters, the fault currents are limited to low values, thus minimizing the hazard of the superconductor going 'normal'. Although a dc superconducting cable may be the most suitable choice for long-distance, high-power transmission of electrical energy, the electrical performance of the dc superconducting cable under commercial operating conditions should be thoroughly investigated.

Unlike normal (copper or aluminum) conductors, a superconductor has no tolerance for temporary overcurrent conditions; if the current exceeds the critical current limit of the superconductor, it will go 'normal' and may be severely damaged. A fault in the cable system, e.g., a

flashover of an insulator at the inverter end, will cause the cable current to rise. The cable may go ‘normal’ if the fault current exceeds the critical current of the superconductor. Therefore, one needs to estimate the magnitude and duration of the fault current.

Although there are no eddy-current and hysteresis losses in the superconducting tapes for operation in a dc system, such losses will be encountered in an actual system because of the presence of current harmonics generated by power conversion at either end of the cable. Therefore, it is essential to know the magnitude of the harmonic currents to assess the ac losses of the cable.

The magnitude and duration of fault currents and the magnitude of the harmonic currents were investigated for two possible applications in Tennessee: (1) a 100-km long, 3-GW cable in the Tennessee Valley Authority (TVA) region, and (2) a 500-m long 500-MW cable in the Nashville Electric Service (NES) region.

II. DESIGNS OF THE CABLES

Initially, two types of dielectric design were considered: (1) cold-dielectric design, and (2) warm-dielectric design. The warm-dielectric design was rejected because of the following reasons:

1. Two separate cables with warm dielectric will be required to complete the electrical circuit as compared with one coaxial cable with the cold dielectric design.
2. The warm-dielectric design will produce magnetic fields in the area surrounding the cables. The cold-dielectric coaxial design will have no external magnetic field.
3. The electric strength and life expectancy of the cold dielectric will be higher than that of the warm dielectric.

The basic assumptions were the following:

1. YBCO (Yttrium Barium Copper Oxide) high-temperature superconductor (HTS) tapes will be used. The tape dimensions are: average width=4.1 mm; average thickness=0.3 mm; steady-state rating=400 A/tape @66 K. Two layers of tapes will be wound with opposite pitch angle, the pitch angle being 20 degrees.

2. Wall thickness of stainless steel tubes=1/8 inch=3.17mm

3. Cryogen flow cross-section=2 square inch=1290.32 mm²

4. Thickness of thermal insulation (vacuum space)=1 inch=25.4 mm

5. Maximum steady-state electric field in dielectric, $E_{max}=20$ kV/mm

The cable systems were designed with two design options, each with two possible voltage ratings. The first design (base design) is based on the premise that the

SUPPLY LN₂ (liquid nitrogen) flows through the central canal of the support former for the cable and the RETURN LN₂ flows in an annulus surrounding the dielectric (Fig. 1). In this design, the SUPPLY LN₂ stream is at high voltage. High-voltage bushings will be required at each refrigeration station for the cooling of the cryogen. The second design (Demko design) is based on the premise that both the SUPPLY and RETURN LN₂ streams will be on the grounded side of the dielectric (Fig. 2). This design will eliminate the high-voltage bushings at each refrigeration station for the SUPPLY LN₂ to circulate. The cryogenic system was designed based on [1].

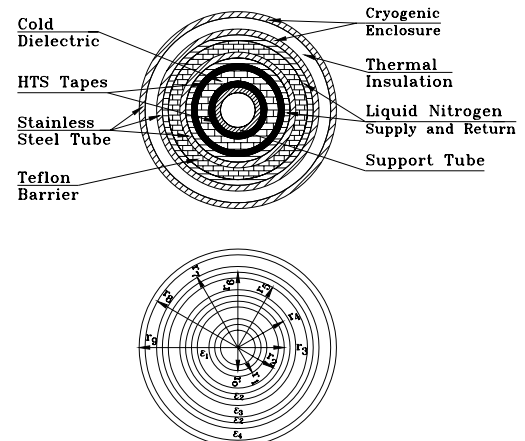


Fig. 1 Cross-sectional view of dc superconducting cable: Base design. r_0 = outer radius of support tube; r_1 = inner radius of dielectric = r_0 + thickness of two layers of HTS tape; r_2 = outer radius of dielectric; r_3, r_4 = inner and outer radii of RETURN LN₂ annulus; r_5, r_6 = inner and outer radii of the annulus of cryogenic envelop; r_7 = outer radius of steel pipe; ϵ_1 = permittivity of dielectric; ϵ_2 = permittivity of LN₂; ϵ_3 = permittivity of thermal insulation

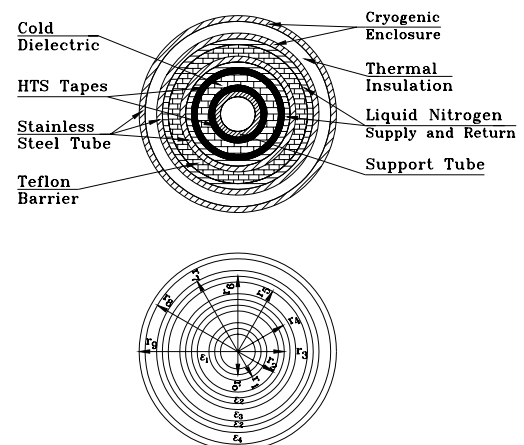


Fig. 2 Cross-sectional view of dc superconducting cable: Demko design. r_0 = outer radius of support tube; r_1 = inner radius of dielectric = r_0 + thickness of two layers of HTS tape; r_2 = outer radius of dielectric; r_3, r_4 = inner and outer radii of SUPPLY LN₂ annulus; r_5 = outer radius of Teflon tube 1 = inner radius of RETURN LN₂ annulus; r_6 = outer radius of RETURN LN₂ annulus; r_7 = outer radius of Teflon tube 2 = inner radius of annulus of cryogenic envelop; r_8 = outer radius of annulus of cryogenic envelop = inner radius of steel pipe; r_9 = outer radius of steel pipe; ϵ_1 = permittivity of dielectric; ϵ_2 = permittivity of LN₂; ϵ_3 = permittivity of Teflon; ϵ_4 = permittivity of thermal insulation

A. 3-GW Cables

For the 3-GW system, the (n-1)-contingency rule was applied. This contingency rule requires that 3 GW of power must be transported by multiple cables, and that if one of the cables is out of service, then the remaining cables must carry the full 3-GW load.

Three alternative designs were studied to satisfy the contingency requirement: 1. one 3-GW cable, 2. three 1.5-GW cables, and 3. four 1-GW cables. The 3-GW cable was designed for the purpose of reference. Of course, two 3-GW cables would have satisfied the contingency requirement. However, it may not be economically viable to design a 6-GW system to transmit only 3-GW power during normal operation. The dimensions of the cables for the base design and different contingency options are shown in Table I, and for the Demko design in Table II.

B. 500-MW Cables

The 500-MW cable is only 500-m long. Its possible application is in a tunnel underneath railroad tracks in Nashville. It has no requirement for contingency. Therefore, one 500-MW cable was designed for two possible voltage ratings for each of the base and Demko designs. The dimensions are shown in Tables III and IV.

III. ANALYSIS AND RESULTS

A. Fault Currents

The most severe fault current through the dc cable will occur if the line-end bushing of the inverter-side smoothing reactor flashes over (Fig. 3). The fault current will consist of two components. The first component will be a traveling wave caused by the discharge of the cable capacitance. The second component will be driven by the voltage source on the ac side of the rectifier.

The magnitude and duration of the cable discharge current cannot be controlled by any external means, such as valve control of the converter or a dc circuit breaker. The second component can be controlled by these external means, and the fault current profile will depend upon the characteristics of the fault interrupter. The fault current analysis followed the techniques proposed in [2].

Discharge Current of the DC Cable

A rectangular traveling current wave, I_d , will be generated at the flashover point at the instant of flashover. This current wave will travel along the cable until it encounters a discontinuity at the rectifier-end smoothing reactor. Part of this current will penetrate the rectifier-end smoothing reactor and the rest will be reflected back to the cable. Because of the large impedance of the smoothing reactor relative to the surge impedance of the cable, most of the current will be reflected back to the cable, i.e., $I_r = -I_d$.

This reflected current wave will travel back along the cable towards the fault location, canceling the forward current wave as it progresses. The magnitude and duration of the discharge current at the point of flashover are given by:

$$I_d = \frac{V_{dc}}{Z_c}, \quad (1)$$

$$\text{and, } \tau = \frac{2\ell}{v}, \quad (2)$$

where I_d =discharge current, V_{dc} =dc voltage of the cable,

$$Z_c = \sqrt{\frac{L}{C}} = \text{surge impedance of the cable, } \tau = \text{duration of}$$

the discharge current at the flashover point, ℓ = cable length, v =velocity of propagation of the current wave in the cable, and L and C =inductance and capacitance per meter of cable. The duration of the discharge current diminishes monotonically along the cable and is zero at the rectifier end.

Component of Fault Current Caused by AC-Side Voltage

This second component of fault current will be maintained by the voltage sources on the ac side of the rectifier. Therefore, the ac-side reactances, the smoothing reactor and the cable reactance will limit this component of the fault current.

The following assumptions were made:

1. Fault current is initiated at the beginning of commutation.
2. There is no commutation overlap.
3. Fault current is interrupted by blocking the firing of the subsequent valves.
4. Firing angle delay is zero
5. Converters operate in 12-pulse mode.
6. AC network reactance beyond the rectifier transformer is negligible.

The 12-pulse system and its equivalent circuit for the computation of the fault current are shown in Fig. 4.

If the fault starts when the reference valve comes into conduction, the fault current will continue to increase until the ac voltage in the loop is zero, even if the sensing system is fast enough to block the next valve. The fault current will then decrease, becoming zero when $\int v dt = 0$. If the next valve is not blocked, then the fault current will continue to rise until the new voltage around the loop is zero. Similarly, as the subsequent valves are not blocked, the fault current will continue to rise.

The voltage across the 12-pulse rectifier bridge and the fault-current profile are shown in Fig. 5. The peak of the fault current is given by:

$$i_{mn} = \frac{(n_m + 1)(A_{11} + A_{21}) + A_{12} + A_{22}}{L_{total}} \quad (3)$$

TABLE I
DIMENSIONS OF CABLES FOR 3-GW SYSTEM: BASE DESIGN

V _{dc} kV	No. of Tapes/Layer	r ₀ mm	r ₁ mm	r ₂ mm	r ₃ mm	r ₄ mm	r ₅ mm	r ₆ mm	r ₇ mm
<i>No Contingency: One 3-GW Monopolar Cable</i>									
200	19	23.44	24.04	36.44	37.04	42.22	45.40	70.80	73.97
300	13	23.44	24.04	44.87	45.47	49.78	52.95	78.35	81.53
<i>Single Contingency: Three 1.5-GW Monopolar Cables</i>									
100	19	23.44	24.04	29.60	30.20	36.37	39.54	64.94	68.12
150	13	23.44	24.04	32.84	33.44	39.10	42.28	67.68	70.85
<i>Single Contingency: Four 1.0-GW Monopolar Cables</i>									
75	17	23.44	24.04	28.10	28.70	35.13	38.31	63.71	66.88
100	13	23.44	24.04	29.60	30.20	36.37	39.54	64.94	68.12

TABLE II
DIMENSIONS OF CABLES FOR 3-GW SYSTEM: DEMKO DESIGN

V _{dc} kV	No. of Tapes/Layer	r ₀ mm	r ₁ mm	r ₂ mm	r ₃ mm	r ₄ mm	r ₅ mm	r ₆ mm	r ₇ mm	r ₈ mm	r ₉ mm
<i>No Contingency: One 3-GW Monopolar Cable</i>											
200	19	13.19	13.79	28.48	29.08	35.44	43.29	47.80	50.98	76.38	79.55
300	13	9.03	9.63	45.73	46.33	50.57	58.42	61.83	65.01	90.41	93.58
<i>Single Contingency: Three 1.5-GW Monopolar Cables</i>											
100	19	13.19	13.79	19.82	20.42	28.77	36.62	41.85	45.03	70.43	73.60
150	13	9.03	9.63	20.98	21.58	29.61	37.46	42.59	45.76	71.16	74.34
<i>Single Contingency: Four 1.0-GW Monopolar Cables</i>											
75	17	11.81	12.41	16.78	17.38	26.70	34.55	40.06	43.23	68.63	71.81
100	13	9.03	9.63	16.18	16.78	26.31	34.16	39.72	42.90	68.30	71.47

TABLE III
DIMENSIONS OF A 500-MW MONOPOLAR CABLE: BASE DESIGN

V _{dc} kV	No. of Tapes/Layer	r ₀ mm	r ₁ mm	r ₂ mm	r ₃ mm	r ₄ mm	r ₅ mm	r ₆ mm	r ₇ mm
50	13	23.44	24.04	26.68	27.28	33.98	37.16	62.56	65.73
100	7	23.44	24.04	29.60	30.20	36.37	39.54	64.94	68.12

TABLE IV
DIMENSIONS OF A 500-MW MONOPOLAR CABLE: DEMKO DESIGN

V _{dc} kV	No. of Tapes/Layer	r ₀ mm	r ₁ mm	r ₂ mm	r ₃ mm	r ₄ mm	r ₅ mm	r ₆ mm	r ₇ mm	r ₈ mm	r ₉ mm
50	13	9.03	9.63	12.48	13.08	24.12	31.97	37.85	41.03	66.43	69.60
100	7	4.86	5.46	13.64	14.24	24.77	32.62	38.40	41.58	66.98	70.15



Fig. 3 Flashover of line-end bushing of inverter-side smoothing reactor

where n_m =number of misfire of the valves in the rectifier bridge, $L_{total} = L_c + L_s + L_\ell$ and the areas, A_{11} , A_{21} , A_{12} and A_{22} are shown in Fig. 5. The details of the analysis are given in [2,3]. The fault current profiles for the 3-GW, 200-kV base design are shown in Fig. 6. The discharge currents, the peak fault currents and their durations are tabulated in Tables V to VIII for both the 3-GW and 500-MW systems for all the design alternatives.

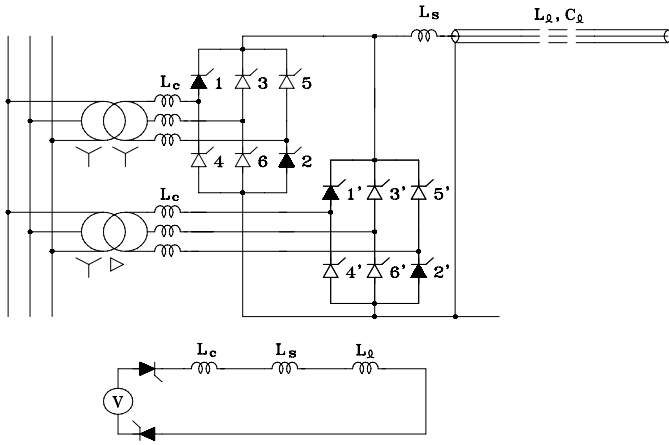


Fig. 4 Representation of a 12-pulse parallel-connected rectifier bridge with fault at inverter end. L_c =commutating inductance; L_s =smoothing inductance; L_ℓ, C_ℓ = inductance and capacitance of the cable

These fault current magnitudes and durations are typically less than that of an ac cable where fault currents can reach 50 kA or more and durations can be 5 – 15 cycles.

B. Harmonic Currents

The source of harmonics in the dc cable are the converters at either end of the cable. The converters are considered to be the voltage sources for the dc-side harmonics. The computation of the harmonics in the 3-GW 100-km cable was based on the standing-wave theory of long transmission lines. For the 500-MW, 500-m cable, the cable was represented as a π -network. It was assumed that the dc cable was terminated at either end by smoothing reactors, L_s . No other filter network was connected to the cable. The equivalent circuits for the long and short cables are shown in Fig. 7.

For the long cable (3-GW, 100-km), the harmonic voltages generated at either end will be attenuated by the smoothing reactors, L_s , and will travel along the cable in opposite directions with almost no attenuation but changing phase. They will be reflected by the reactors repeatedly as they travel back and forth along the cable. The magnitude of a harmonic at any point along the cable will be the algebraic sum of these two components. As a result, the harmonic voltage or current level will exhibit standing wave patterns with successive maxima and minima. The maxima occur when these two components are in phase, minima when they are out of phase by π radians.

The details of the analysis have been discussed in [2,4]. The magnitudes and phase angles of the generated harmonic voltages, V_1 and V_2 , will generally be different. As the ac systems on either side of the dc system are asynchronously connected, the phase angles will vary at random. Computations were made for the cases when the two harmonic voltage sources are equal in magnitude (i.e., the ac system voltages feeding the rectifier and

inverter are equal), but differ in phase angle, δ , by 0 and π . The equations for the harmonic currents are given by:

$$I_{\max} = \frac{V_n}{2\pi f_n L_s \sin(\beta \ell / 2)}, \quad \text{for } \delta=0 \quad (4a)$$

$$I_{\max} = \frac{V_n}{2\pi f_n L_s \cos(\beta \ell / 2)}, \quad \text{for } \delta=\pi \quad (4b)$$

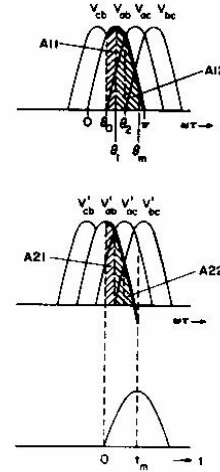


Fig. 5 Voltage across 12-pulse rectifier bridge and current profile under fault condition

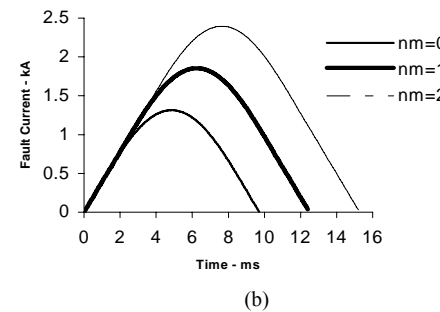
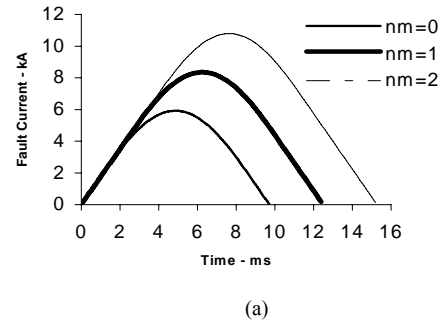


Fig. 6 Fault current profiles of the 3-GW, 200-kV 100-km long base design. 12-pulse converter bridge connected in parallel; Commutating reactance=0.15 p.u.; (a) Smoothing reactor, $L_s=100$ mH; (b) Smoothing reactor, $L_s=500$ mH

TABLE V
 FAULT CURRENTS IN 3-GW 100-kM SYSTEM: BASE DESIGN
 Commutating reactance=0.15 p.u.; $p_n=12$; $n_m=1$

Rated Voltage kV	Cable Inductance nH/m	Cable Capacitance nF/m	Smoothing Inductance mH	Discharge Current		Fault Current	
				Peak kA	Duration ms	Peak kA	Duration ms
<i>No Contingency i.e., One 3-GW Monopolar Cable</i>							
200	83.19	0.3339	100	12.67	1.054	8.352	12.5
			250			3.609	
			500			1.854	
300	124.8	0.2226	100	12.67	1.054	11.387	12.5
			250			5.188	
			500			2.720	
<i>Single Contingency i.e., Three 1.5-GW Monopolar Cables</i>							
100	41.6	0.6678	100	12.67	1.054	4.451	12.5
			250			1.854	
			500			0.939	
150	62.4	0.4452	100	12.67	1.054	6.339	12.5
			250			2.720	
			500			1.394	
<i>Single Contingency i.e., Four 1-GW Monopolar Cables</i>							
75	31.2	0.8904	100	12.67	1.054	3.386	12.5
			250			1.398	
			500			0.707	
100	41.6	0.6678	100	12.67	1.054	4.392	12.5
			250			1.843	
			500			0.937	

TABLE VI
 FAULT CURRENTS IN 500-MW 500-M SYSTEM: BASE DESIGN
 Commutating reactance=0.15 p.u.; $p_n=12$; $n_m=1$

Rated Voltage kV	Cable Inductance nH/m	Cable Capacitance nF/m	Smoothing Inductance mH	Discharge Current		Fault Current	
				Peak kA	Duration μ s	Peak kA	Duration ms
50	20.8	1.336	100	12.67	5.27	2.283	12.5
			250			0.936	
			500			0.472	
100	41.60	0.6678	100	12.67	5.27	4.057	12.5
			250			1.782	
			500			0.921	

where

- V_n =generated harmonic voltage, V
- f_n =harmonic frequency, Hz
- L_s =inductance of smoothing reactor, H
- $\beta=2\pi f_n/v_c$, rad/m
- v_c =velocity of propagation in cable, m/s
- ℓ =length of cable, m.

The results are shown in Tables IX for the base design. As the magnitudes of the current harmonics are independent of the cable dimensions, for a given cable length, the magnitudes of the current harmonics for the Demko design are the same as in Table IX. The ripple losses at 720 Hz (12th harmonic) were computed for the worst case for each design, i.e., highest ripple currents and lowest smoothing inductance. The monoblock model was used [5,6] The monoblock model assumes

TABLE VII
 FAULT CURRENTS IN 3-GW 100-kM SYSTEM: DEMKO DESIGN
 Commutating reactance=0.15 p.u.; $p_n=12$; $n_m=1$

Rated Voltage kV	Cable Inductance nH/m	Cable Capacitance nF/m	Smoothing Inductance mH	Discharge Current		Fault Current	
				Peak kA	Duration ms	Peak kA	Duration ms
<i>No Contingency i.e., One 3-GW Monopolar Cable</i>							
200	145.0	0.1915	100	7.268	1.054	7.557	12.5
			250			3.452	
			500			1.811	
300	311.5	0.0892	100	5.075	1.054	9.088	12.5
			250			4.652	
			500			2.565	
<i>Single Contingency i.e., Three 1.5-GW Monopolar Cables</i>							
100	72.52	0.3831	100	7.268	1.054	4.215	12.5
			250			1.811	
			500			0.928	
150	155.8	0.1783	100	5.075	1.054	5.556	12.5
			250			2.565	
			500			1.352	
<i>Single Contingency i.e., Four 1-GW Monopolar Cables</i>							
75	60.44	0.4596	100	6.541	1.054	3.221	12.5
			250			1.369	
			500			0.699	
100	103.8	0.2675	100	5.075	1.054	4.001	12.5
			250			1.771	
			500			0.918	

TABLE VIII
 FAULT CURRENTS IN 500-MW 500-M SYSTEM: DEMKO DESIGN
 Commutating reactance=0.15 p.u.; $p_n=12$; $n_m=1$

Rated Voltage kV	Cable Inductance nH/m	Cable Capacitance nF/m	Smoothing Inductance mH	Discharge Current		Fault Current	
				Peak kA	Duration μ s	Peak kA	Duration ms
50	51.92	0.535	100	5.08	5.27	2.282	12.5
			250			0.936	
			500			0.472	
100	103.8	0.268	100	5.08	5.27	4.056	12.5
			250			1.781	
			500			0.921	

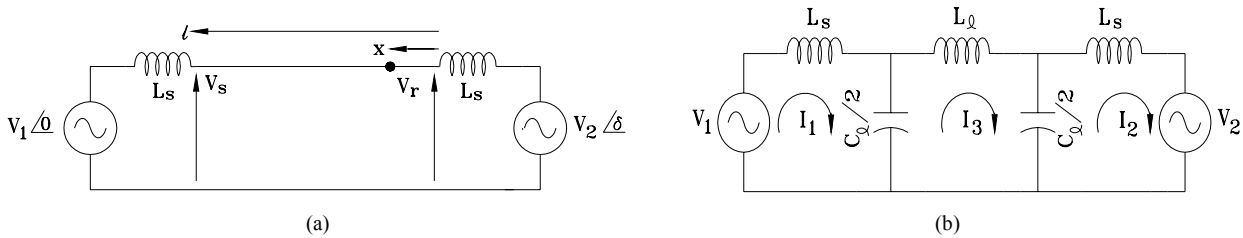


Fig. 7 Schematic representations of the dc cable system for harmonic analysis. (a) 3-GW, 100-km cables; (b) 500-MW, 500-m cables
 V_1, V_2 = harmonic voltage sources; L_s = smoothing reactors; L_ℓ, C_ℓ = total inductance and capacitance of cable

that the HTS is not fully penetrated and that the ac losses are the same for this condition whether there is a dc transport current or not. In reality, the harmonic losses will even be lower when the superimposed dc transport is considered [7]. For the short cable (500-MW, 500-m), as shown in Fig. 7(b), the current, I_3 , through L_c is the harmonic current in the cable. Filter capacitances can be incorporated into the admittances, if necessary. The equation for I_3 is given by [2]:

$$I_3 = \frac{V_1 - V_2}{4\pi f_n L_s \cos^2(\beta\ell/2) + Z_c \sin\beta\ell}, \quad (5)$$

where

V_1, V_2 = generated harmonic voltages at either end of the cable, V

Z_c = surge impedance of the cable, Ω .

Equation (5) shows that if $V_1 = V_2$, no harmonic current will exist. Therefore, computations were made for $V_1 = -V_2$. Results are shown in Table X for the base design. The harmonic current for the Demko design will be practically the same because the term, $Z_c \sin\beta\ell$, in the denominator is negligible for the short length of cable. Because of the significantly smaller harmonic currents of the 500-MW system, the ac losses will be negligible.

IV. DISCUSSION

A. Fault Currents

Higher dc system voltage will increase the discharge current. However, higher system voltage requires thicker insulation between the two coaxial HTS cylinders. Thicker insulation increases the inductance and decreases the capacitance of the cable, thus increasing the surge impedance of the cable. This will tend to decrease the discharge current as shown in (1). In some designs, the discharge current may even decrease for higher system voltage as evident in Tables V - VIII. Similarly, as the fault current is driven by the ac system voltage, the fault current should be higher for higher system voltage. The discharge current is not affected by the terminal (smoothing) inductance because it is confined within the cable and it depends upon the dc voltage and the cable surge impedance. However, the fault current is significantly affected by the terminal inductance because the fault current flows from the ac-side voltage to the point of fault via the commutating inductance of the converter transformer, the terminal inductance and the cable inductance. One misfire ($n_m=1$) of the converter valves was considered to be sufficient delay for the protection system to respond in turning the valves off.

Only one length for each of the two systems was considered, i.e., 100 km for the 3-GW system and 500 m for the 500-MW system. The duration of the discharge current is directly proportional to the cable length. The magnitude of the discharge current is independent of the

length. However, the peak of the fault current will be reduced for longer length because the increased cable inductance will provide higher impedance to the flow of the fault current. As the terminal inductance is significantly higher than the cable inductance, the effect of the cable length on the fault current will not be significant.

Neither the durations nor the magnitudes of the discharge currents and the fault currents are high enough to damage the superconducting cables which would be wound with HTS tapes stabilized with a normal conductor such as copper or brass [8,9].

B. Harmonic Currents

It should be observed in Tables IX and X that lower dc voltages of the cable produce lower harmonic currents. Lower dc voltage means lower ac-side voltage. As these ac voltages are the sources of harmonics (both voltage and current), lower dc rated voltage of the cable will produce lower harmonic current. It should also be noticed in these Tables that higher smoothing inductances at the converter terminals lower the harmonic current for the same dc voltage. This is caused by higher voltage drop across the higher smoothing inductances.

The level of ac losses due to harmonic currents in the dc cables do not pose any problem for the reliable operation of the dc cables [10]. The ac losses due to the harmonic currents (Table IX) are much less than the thermal heat in-leak to the cryostat which is on the order of 3-5 W/m. This means that dc harmonic filters will not be required. It will lower the cost of the converters a little and also increase the reliability of operation by eliminating some accessories in the system.

C. Comparison between Base Design and Demko Design

The base design (Fig. 1) is a standard design where the SUPPLY stream of the cryogen flows through the core of the cable assembly and the RETURN stream envelops thesecond concentric HTS cylinder. This is very desirable for cryogenic considerations because of its ability to cool the cable system uniformly. The SUPPLY stream of cryogen is enclosed inside the high-voltage HTS cylinder. This SUPPLY stream of cryogen has to be taken out of the cable system at every refrigeration station for recirculation and cooling. This means that the SUPPLY stream has to penetrate through the high-voltage envelop to be delivered to the refrigeration system which is at ground potential. This can be done by designing a high-voltage bushing to be placed at each station of the refrigeration system. It will be expensive and a potential source of unreliability due to thermal, mechanical and electric stresses.

TABLE IX
CURRENT HARMONICS IN 3-GW 100-kM SYSTEM: BASE DESIGN
Firing angle, $\alpha=15^\circ$; Overlap angle, $u=32.55^\circ$
Commutating reactance, $X_c=0.15$ p.u.; Harmonic number, $p_n=12$

DC Voltage kV	Current kA	Smoothing Inductance mH	Harmonic Current, A @		Ripple Losses mW/m @ 66 K
			$\delta=0$	$\delta=180^\circ$	
<i>No Contingency i.e. One 3-GW Monopolar Cable</i>					
200	15	100	34.47	86.64	0.4944
		250	13.79	34.66	
		500	6.89	17.33	
300	10	100	51.70	129.96	3.4615
		250	20.68	51.98	
		500	10.34	25.99	
<i>Single Contingency i.e. Three 1.5-GW Monopolar Cables</i>					
100	15	100	17.23	43.32	0.0618
		250	6.89	17.33	
		500	3.45	8.66	
150	10	100	25.85	64.98	0.4325
		250	10.34	25.99	
		500	5.17	13.00	
<i>Single Contingency i.e. Four 1-GW Monopolar Cables</i>					
75	13.33	100	12.93	32.49	0.0323
		250	5.17	13.00	
		500	2.59	6.50	
100	10	100	17.23	43.32	0.1281
		250	6.89	17.33	
		500	3.45	8.66	

TABLE X
CURRENT HARMONICS IN 500-MW 500-M SYSTEM: BASE DESIGN
Firing angle, $\alpha=15^\circ$; Overlap angle, $u=32.55^\circ$
Commutating reactance, $X_c=0.15$ p.u.; Harmonic number, $p_n=12$

DC Voltage kV	Current kA	Smoothing Inductance mH	Harmonic Current A
50	10	100	8.01
		250	3.20
		500	1.60
100	5	100	16.01
		250	6.40
		500	3.20

In contrast, both the cryogen streams are at ground potential under steady-state operation in the Demko design (Fig. 2). From electrical standpoint, this design will be simpler, cost effective and more reliable. The discharge current during fault of the Demko design (Tables VII and VIII) is smaller than that of the base design (Tables V and VI) because of the higher surge impedance of the Demko design, as shown in (1). The fault component of the current

for the Demko design is also somewhat lower than that for the base design because of the higher inductance of the Demko design as shown in (3).

The harmonic currents for the base and the Demko designs were found to be the same for both the 100-km and 500-m cables. For the long cables, as shown in (4), the harmonic current is a function of the smoothing inductance, L_s , and the propagation constant, β for given harmonic

voltage, V_n and harmonic frequency, f_n . β is a function of the permittivity of the cable dielectric. Therefore, for the same cable length, terminal inductance and the dielectric, the harmonic currents for the two designs must be the same. For short cables, as (5) shows, the harmonic current is a function of the surge impedance of the cable. However, the term, $\sin\beta\ell$, is very small, and therefore does not affect the magnitude of the harmonic currents.

V. CONCLUSIONS

Neither fault current nor current harmonics will impact the steady-state operation or degrade the performance of the dc superconducting cable.

The Demko design with both GO and RETURN flows of the cryogen on the grounded side of the cable system will enhance the reliability as well as the cost effectiveness of the cable system. Further study is needed to optimize this design

VI. REFERENCES

- [1] J.A. Demko, et al., "Cryostat Vacuum Thermal Considerations for HTS Power Transmission Cable Systems", *IEEE Transactions on Applied Superconductivity*, Vol. 13, No. 2, pp. 1930-1933, June 2003.
- [2] P. Chowdhuri and H.L. Laquer, "Some Electrical Characteristics of a dc Superconducting Cable", *IEEE Transactions on Power Apparatus and Systems*, Vol. PAS-97, No. 2, pp. 99-408, 1978.
- [3] H.A. Peterson, A.G. Phadke and D.K. Reitan, "Transients in EHVDC Power Systems: Part I – Rectifier Fault Currents", *IEEE Transactions on Power Apparatus and Systems*, Vol. PAS-88, pp. 981-989, 1969.
- [4] D.H. Welle, A.G. Phadke and D.K. Reitan, "Evaluation of Harmonic Levels on an HVDC Transmission Line", *Proc. American Power Conference*, Vol. 29, pp. 1100-1108, 1967.
- [5] J.J. Rabbers: AC loss in Superconducting Tapes and Coils. Proefschrift Universitaet Twente, Enschede, The Netherlands, 2001
- [6] V. Minervini, "Two-Dimensional Analysis of AC Loss in Superconductors carrying Transport Current", *Advances in Cryogenic Engineering Materials*, Vol. 28, pp. 587-599, 1982.
- [7] B. des Ligneris, et al., "Decrease of AC Losses in High Tc Superconducting tapes by Application of a DC Current", *Advances in Cryogenic Engineering Materials*, Vol. 46, pp. 831-837, 2000.
- [8] J.W. Lue et al., "Fault Current Tests of a 5-m HTS Cable", *IEEE Transactions on Applied Superconductivity*, Vol. 11, No. 1, pp. 1785-1788, 2001.
- [9] J.W. Lue, M.J. Gouge and R.C. Duckworth, "Over-current Testing of HTS Tapes", *IEEE Transactions on Applied Superconductivity*, to be published in Vol. 15.
- [10] J.A. Demko, et al., "Practical AC Losses and Thermal Considerations for HTS Power Transmission Cable Systems", *IEEE Transactions on Applied*

Superconductivity, Vol. 11, No. 1, pp. 1789-1792, March 2001.

Pritindra Chowdhuri (M'52-SM'60-F'96) received B.Sc. in physics and M.Sc. in applied physics from Calcutta University, India, M.S. in electrical engineering from Illinois Institute of Technology and D.Eng. in engineering science from Rensselaer Polytechnic Institute.

He has worked with Westinghouse Electric Corp., East Pittsburgh, Maschinenfabrik Oerlikon, Zurich, Switzerland, Forschungskommission des SEV and VSE fuer Hochspannungsfragen, Daeniken, Switzerland, General Electric Co., Pittsfield, MA, Schenectady, NY, Erie, PA and Los Alamos National Laboratory, Los Alamos, NM. He joined the Center for Electric Power, Tennessee Technological University as professor of electrical engineering in 1986.

Dr. Chowdhuri is a Fellow of the Institution of Electrical Engineers (U.K.), the American Association for the Advancement of Science and the New York Academy of Science. He is a member of the Power Engineering Society, Industry Applications Society, Electromagnetic Compatibility Society and the Dielectrics and Electrical Insulation Society of the IEEE. He is also a member of CIGRE, Paris, France. He is a registered professional engineer in Massachusetts.

Chandralekha Pallem (Student Member'02) received B.Eng. in electrical engineering from Jawaharlal Nehru Technological University, India and M.S. in electrical engineering from Tennessee Technological University. She is working for her Ph.D. at Tennessee Technological University. Her primary areas of interest are electric power systems and high voltage engineering.

Jonathan A. Demko received B.S., M.S. and Ph.D. in mechanical engineering from Texas A & M University.

He has over 18 years of experience in the thermal-fluids and thermal management areas. He worked for General Dynamics/Fort Worth (currently Lockheed Martin Tactical Aircraft Systems) as the Thermodynamics Analysis Group Lead Engineer and Thermal Management Team Leader for the National Aerospace Plane (NASP) program. He also held engineering positions with the Superconducting Super Collider Laboratory Cryogenics Department. He was a Senior Member of the Technical Staff at Sandia National Laboratory. At present, he is with Oak Ridge National Laboratory where he is involved with the development of electric power applications (power cables and transformers) of high temperature superconductors.

Dr. Demko is a member of the American Society of Mechanical Engineers (ASME) and the Cryogenic Society of America (CSA). He is a registered professional engineer in Texas.

Michael J. Gouge received B.S. in physics with honors from the United States Naval Academy, Ph.D. in physics from University of Tennessee, Knoxville, TN.

He has been at Oak Ridge National Laboratory since 1986 working on energy programs involving cryogenic and superconducting technology. He is now leader of the Applied Superconductivity Group at Oak Ridge National Laboratory His group presently is involved with high temperature superconducting (HTS) cables, transformers and generators as well as quench and stability, ac-loss and other studies of HTS conductors and coils. Included in this R & D program is optimization of cryogenic cooling systems for these emerging technologies.

